Eur Biophys J (1984) 11:3–15

European Biophysics Journal

The spatial structure of the axially bound methionine in solution conformations of horse ferrocytochrome c and *Pseudomonas aeruginosa* ferrocytochrome c 551 by ^{1}H NMR

H. Senn, M. Billeter, and K. Wüthrich

Institut für Molekularbiologie und Biophysik, Eidgenössische Technische Hochschule Hönggerberg, CH-8093 Zürich, Switzerland

Received March 5, 1984/Accepted May 10, 1984

Abstract. A generally applicable method for the determination of the spatial structure of the heme iron-bound methionine in c-type ferrocytochromes at atomic resolution is presented. It relies primarily on measurements of nuclear Overhauser effects between the individual hydrogen atoms of the axial methionine, and between individual hydrogens of the methionine and the heme group. Four different methionine conformers, corresponding to the four possible stereospecific assignments for the methionine methylene proton resonances, are generated by a structural interpretation of the nuclear Overhauser effects with the use of an interactive computer graphics technique. A unique structure and unique stereospecific resonance assignments are then obtained by discriminating between these four conformers on the basis of van der Waals' constraints and heme ring current effects on the chemical shifts. The use of the method is illustrated with studies of horse ferrocytochrome c and *Pseudomonas aeruginosa* ferrocytochrome c 551. Comparison with the crystal structures shows close coincidence between the methionine conformations in solution and in single crystals of these proteins.

Key words: Cytochrome c, nuclear magnetic resonance, protein conformation, heme iron coordination, nuclear Overhauser effect

Introduction

Recent studies of the heme iron coordination in the solution conformations of a selection of mitochondrial and bacterial cytochromes c (Senn et al. 1980, 1983a, 1983b; Keller et al. 1980; Senn and Wüthrich 1983a, 1983b, 1983c) have shown a dominant influence of the spatial arrangement of the axial methionine on the electronic structure of heme c in the oxidized proteins. In previous investigations four different structure types have been qualitatively characterized. Here we describe a method that enables determination of the spatial structure of the axial methionine in solutions of reduced cytochromes c at atomic resolution and apply this technique to two proteins which represent two of the four structure types.

The present structure determination relies on the use of NMR for measurements of NOE's between hydrogen atoms of the axial methionine and heme c, and of ring current shifts of the methionine protons due to the heme group. For the structure determination an interactive computer graphics technique is used. A crucial aspect is that sufficient data could be collected to overcome the inherent limitations for determination of amino acid side chain conformations which arise because stereoselective resonance assignments cannot usually be obtained by ^{1}H-NMR alone (Wüthrich et al. 1983).

Theory

The present study exploits the correlations between NOE's and intramolecular ^{1}H-^{1}H distances. The NOE is the fractional change in intensity by cross-relaxation of one NMR line when another resonance is irradiated with a radiofrequency field. The extent of this change is related to the distance between the observed spin and the irradiated spin. However, when working with macromolecules at high magnetic fields, the correlations between NOE intensity and ^{1}H-^{1}H distances may be masked by spin diffusion, so that special precautions must be taken. The fundamental aspects have in the past been analyzed (Solomon 1955; Noggle and Schirmer 1971; Kalk and Berendsen 1976; Bothner-By and Noggle 1979) and

Abbreviations: NMR, nuclear magnetic resonance; NOE, nuclear Overhauser effect; TOE, truncated driven nuclear Overhauser effect

the situation in proteins, as it is encountered in the present work, has recently been extensively discussed (Gordon and Wüthrich 1978; Wagner and Wüthrich 1979; Dubs et al. 1979; Anil Kumar et al. 1981; Keller and Wüthrich 1981; Dobson et al. 1982).

Intramolecular ^{1}H-^{1}H distances were derived from truncated driven NOE (TOE) experiments. The time-dependence of the magnetization of the nonirradiated spins i in a TOE experiment is determined by

$$\frac{dM_i}{dt} = -\varrho_i M_i - \sum_{j \neq i} \sigma_{ij} M_j \,, \tag{1}$$

where M_i is the difference between the actual magnetization M_{zi} of spin i and its equilibrium magnetization M_i^0. The quantities ϱ_i and σ_{ij} determine the spin-lattice relaxation and the cross-polarization, respectively,

$$\varrho_i = \frac{\hbar^2\gamma^4}{10} \sum_{j \neq i} \frac{1}{r_{ij}^6} \left[\tau_c + \frac{3\,\tau_c}{1 + (\omega\tau_c)^2} \times \frac{6\,\tau_c}{1 \times 4\,(\omega\tau_c)^2} \right], \tag{2}$$

and

$$\sigma_{ij} = \frac{\hbar^2\gamma^4}{10} \frac{1}{r_{ij}^6} \left[\frac{6\,\tau_c}{1 + 4\,(\omega\tau_c)^2} - \tau_c \right], \tag{3}$$

where ω is the Larmor frequency, r_{ij} the distance between spins i and j, $2\pi\hbar$ the Planck constant, γ the gyromagnetic ratio, and τ_c the effective rotational correlation time. To describe the situation which results from selective irradation of a proton in a protein, we denote as spin 1 the irradiated nucleus, as spin 2 the observed nucleus and as spins i all the other protons in the molecule. We further assume that at the outset of the experiment spin 1 attains instantaneously the equilibrium magnetization M_1^0, which does not affect the conclusions in the present study (for a more detailed discussion of the initial time-course of the magnetization of spin 1 see Wagner and Wüthrich 1979). In the early phase of the experiment, $M_1 = M_1^0$, $M_2 = M_i = 0$ and Eq. (1) can be rewritten for short times, τ, as

$$M_2(\tau) = -\sigma_{21} M_1^0 \tau \,. \tag{4}$$

We conclude from Eqs. (1) and (4) that while at long times M_2 may be affected by cross-relaxation with many nearby protons in the protein, i.e., by "spin diffusion", M_2 at short times is directly related to σ_{21}. In practice, several TOE experiments with truncation after different short time intervals are recorded, so that the "build-up" of M_2 can be followed (see following section).

Equation (3) shows that the cross-relaxation rate σ_{21} obtained experimentally through Eq. (4) depends on the inverse sixth power of the ^{1}H-^{1}H distance, r_{12}^{-6}, and on a function of the effective correlation time, $f(\tau_c)$. Since the latter is not a priori known, we have chosen to calibrate the correlation between σ_{21} and the ^{1}H-^{1}H distances empirically, using the known distance between covalently linked protons as a reference. We further compared the effective correlation times for different groups of covalently linked protons, which provided information on the intramolecular mobility in the heme crevice of the cytochromes c (Olejniczak et al. 1981).

Experimental

Materials

Horse ferricytochrome c "type VI" was purchased from Sigma. *Pseudomonas aeruginosa* ferricytochrome c was obtained as a gift from Dr. I. Gunsalus and Dr. P. Debrunner, University of Illinois, Urbana. The protein concentration in the NMR samples was 0.004 M–0.006 M. The p^{2}H in the ^2H_2O solutions was adjusted by addition of minute amounts of ^{2}HCl or NaO^{2}H. Solutions of the fully reduced form of the cytochromes were obtained by addition of solid sodium dithionite.

NMR measurements

High resolution ^{1}H NMR spectra were recorded in the Fourier mode on a Bruker HX 360 and a Bruker WM 500 spectrometer. TOE difference spectra were obtained as described previously (Dubs et al. 1979; Wagner and Wüthrich 1979), using the pulse sequence

$$[T_D - \tau(\omega_1) - \text{observation pulse} - T_D - \tau(\omega_{\text{off res}}) - \text{obs. pulse}]_n \,. \tag{5}$$

T_D is a delay time allowing the system to return to equilibrium; τ is the time period during which a selective low-power radiofrequency field is applied to proton 1, or off-resonance, respectively and n indicates the number of transients which were accumulated to improve the signal-to-noise ratio. The free induction decays with and without NOEs were stored alternatively in different memory locations and a difference spectrum was obtained by subtracting the free induction decay without NOE from the one with NOE. The NOE build-up rates were studied

by measurements of a series of TOE difference spectra with different irradiation times, which were all short compared to the time needed to reach a steady-state NOE (Noggle and Schirmer 1971). Chemical shifts are in parts per million (ppm) from internal sodium 3-trimethyl-silyl-[2,2,3,3-$^2H_4$]-propionate.

Use of interactive computer graphics for spatial structure determination

For the determination of the spatial structure of the heme-methionine complex an interactive model-building program was used, which allows generation of different conformations by rotations about individual dihedral angles. Diamond's (1978) BILDER program was modified and extended, so that it allows visualization of deviations of proton-proton distances in a molecular structure from predetermined values for these distances derived from the NOE measurements (Billeter 1980). The hardware used consisted of an Evans & Sutherland picture system connected to a PDP 11–34 computer. Deviations between actual and predetermined distances were presented on the screen by flashing arrows defined by the following vector sum:

$$\vec{a_j} = c \sum_i \frac{(\vec{r_i} - \vec{r_j})}{d_{ij}} (d_{ij} - D_{ij}) \qquad (6)$$

$\vec{a}_j$ is the arrow attached to proton j; the index i identifies protons for which the distance to proton j is constrained by an NOE; c is a scaling constant; $\vec{r}_i$ and $\vec{r}_j$ are the coordinate vectors of the individual protons; d_{ij} is the distance between protons i and j in the structure considered; D_{ij} is the distance between protons i and j imposed by the NOE. In the simplest situation, where there is a single NOE constraint between protons i and j, $\vec{a}_i$ will be on a straight line through i and j. The length of the arrow will be small when d_{ij} is close to D_{ij}. The arrows in three dimensions are updated with every change of conformation. The operator's task is to decrease the lengths of all arrows by rotations about the dihedral angles.

In this procedure of fitting the spatial molecular structure to distance constraints imposed by the NOEs, the covalent structure, including the stereochemistry at the iron-bound sulfur atom, was not modified. The location of Met "above" the heme plane (rather than "below" the heme plane), the bond angles and the bond length were taken from the X-ray structures of reduced *Pseudomonas aeruginosa* cytochrome c-551 (Matsuura et al. 1982) and reduced

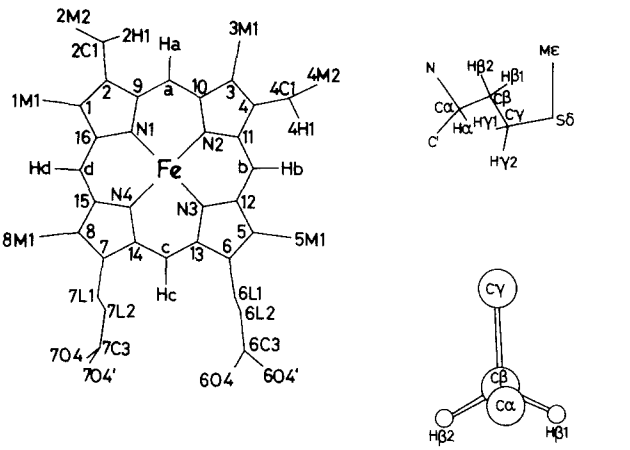

Fig. 1. Nomenclature used for the atoms of heme c and the axial methionine in c-type cytochromes. Heme c: the pyrrole ring carbons are numbered from 1 to 16. Side chain atoms are identified by the number of the pyrrole ring carbon to which the side chain is attached, a letter defining the atom type and the number of heavy atom-heavy atom bonds separating the atom from the pyrrole ring. The pyrrole nitrogens are labelled N1–N4, the methine bridges between the pyrrole rings a–d. Methionine: the IUPAC/IUB convention (1970) is used. Hydrogen atoms are explicitly shown where they could be stereospecifically identified in the ^1H NMR spectra. (The figure in the lower right illustrates the definition of Hβ1 and Hβ2; the definition of Hγ1 and Hγ2 is analogous). Otherwise, methyl groups and methylene groups are replaced by equivalent spheres M and L, respectively. M is located centrally with respect to the three methyl protons and its radius is 1.8 Å. L is located at the position of the methylene carbon and the radius is 1.6 Å. To generate different conformations the following dihedral angles were used: χ^1, χ^2, and χ^3 for methionine, according to the IUPAC/IUB convention, and Ω for rotations about the iron-sulphur bond perpendicular to the heme plane. Ω is defined to be 0 when the C$^\gamma$ of methionine and the N4 of the heme are in a *cis* conformation, and its value increases with clockwise rotations of N4 when looking from the iron towards the sulphur

tuna cytochrome c (Takano and Dickerson 1981), where the latter data were used for the equine protein. The nomenclature for the atoms of heme c and the axial methionine is described in Fig. 1. In addition to the standard torsion angles χ^1, χ^2, and χ^3, a torsion angle Ω is introduced to describe rotations about the iron-sulfur bond. The length of the iron-sulfur bond was taken from the X-ray structures, with this bond oriented perpendicular to the heme plane.

Ring current calculations

Once a conformation was found which satisfied the NOE distance constraints, it was further checked for compatibility with the observed ^1H chemical shifts. For this the ring current shifts for the methionine protons in the NOE structure arising from the proximity to the heme plane were calculated with the

Johnson-Bovey (1958) formalism, with five pairs of "current loops" centered about the heme macrocycle and the four pyrrole rings. The parameters given by Giessner-Prettre and Pullman (1971) were used. This procedure was found in studies with different molecules to give the best agreement between calculated and observed ring current shifts (Perkins 1980).

Computation of van der Waals contacts

The conformers derived from the NOE distance constraints were checked for violations of van der Waals interatomic distances. For this a program was used which attributed specified radii to all atoms in Fig. 1 and computed the overlap of the resulting spheres between any two atoms in the spatial molecular structure.

Results and Discussion

NMR experiments

The 360-MHz spectra of *P. aeruginosa* ferrocytochrome c-551 and horse ferrocytochrome c are shown in Fig. 2. In both spectra the four mesoproton singlet lines of heme c (Fig. 1) are well separated at the low field end of the spectrum between 9.0 and 10.0 ppm, and the ε-methyl and the methylene proton lines of the axial methionine are resolved at the high field end between 0 and −4.0 ppm. As indicated in the figure, the heme meso proton lines were previously individually assigned (Keller and Wüthrich 1978a, b). The C^{β} and C^{γ} methylene resonances were distinguished, but no stereospecific assignments were obtained (Gordon and Wüthrich 1978; Senn et al. 1980). All the experiments described in the following rely on selective irradiation of these well-resolved resonance lines. As an illustration, Fig. 3 shows the TOE difference spectra obtained when the preirradiation was applied on the methionine ε-methyl resonance in horse ferrocytochrome c. In addition to the above-mentionned well resolved resonances, NOE measurements were also obtained for the C^{α} proton of the axial methionine. In Fig. 4A the variations in the intensity of the individual peaks in the TOE difference spectra of Fig. 3 are plotted against τ. Figure 4B shows plots of the corresponding data for *P. aeruginosa* ferrocytochrome c-551.

Similar measurements were made with preirradiation on the individual methylene proton resonances of the axial methionine. As indicated in the captions to Figs. 5 and 6, these experiments were done at 500 MHz, so that the spectral resolution was improved over that in Fig. 2. None the less the data

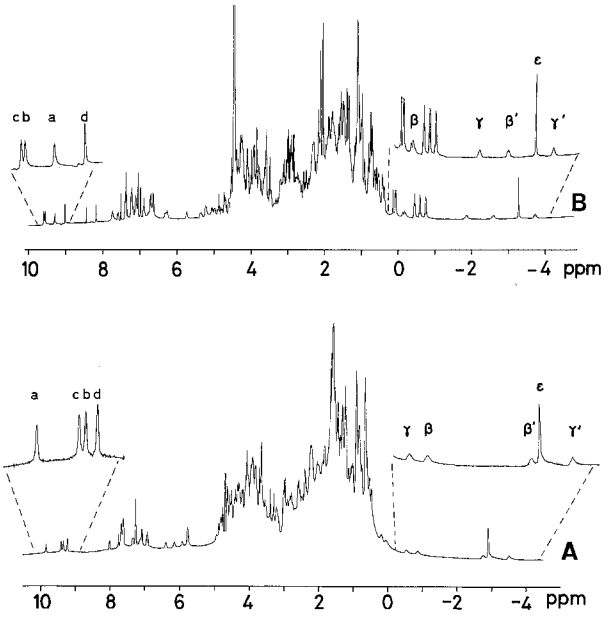

Fig. 2. A ^{1}H-NMR spectrum at 360 MHz of a 0.004 M solution of *P. aeruginosa* ferrocytochrome c-551 in ^2H_2O, p^{2}H 7.5, T = 30° C. **B** ^{1}H-NMR spectrum at 360 MHz of a 0.006 M solution of horse ferrocytochrome c in ^2H_2O, p^{2}H 7.2, T = 53° C. The extreme high and low field regions are also shown on an expanded scale. The individual resonance lines of the heme meso protons are labelled by a–d and the resonance lines of the axial methionine protons with Greek letters (Fig. 1). The higher field line of the two methylene groups is arbitrarily labelled β', and γ', respectively

obtained with preirradiation on H_{β} in horse ferrocytochrome c were not used, since this line is overlapped with an as yet unidentified line, so that side-effects influencing the NOE intensities could not be ruled out. In *P. aeruginosa* ferrocytochrome c-551 the cross-relaxation between H_{β}' and εCH_3 was not further analyzed, since even at 500 MHz the two lines are too close to exclude effects of direct irradiation on one line when the radiofrequency is applied to the other line. Figure 5 shows the build-up curves for the heme c meso protons of both proteins and Fig. 6 those for the hydrogen atoms of the axial methionine. Additional measurements were obtained with irradiation on the heme meso protons. These are not shown here but will be used in the following.

Some important features of the structures determined by the quantitative analysis in the following sections can be anticipated from inspection of the NOE build-up curves in Figs. 4–6. First, we conclude that the methionine side chain is largely immobilized in the proteins, since different NOE's are generally observed for the individual methylene protons. This conclusion receives further support from the observation that the chemical shifts for the individual methylene protons are sizeably different and are nearly independent of temperature between 5° and 70° C (Moore and Williams 1980). Second, Fig. 5

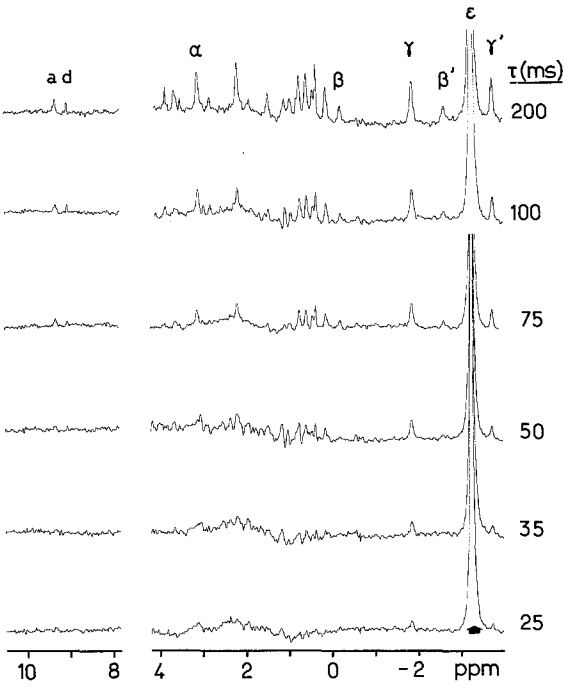

Fig. 3. Truncated driven nuclear Overhauser enhancement (TOE) difference spectra at 500 MHz of horse ferrocytochrome c obtained as the difference between recordings with and without preirradiation on the high-field ε-methyl resonance of the axial methionine (Fig. 2), T = 30° C, p^{2}H 7.2, protein concentration 0.006 M in ^2H_2O. The length of the preirradiation time, τ, is indicated with each trace. Individual resonances of the axial methionine and the heme c are identified with greek letters and with the letters a and d, respectively (Fig. 1)

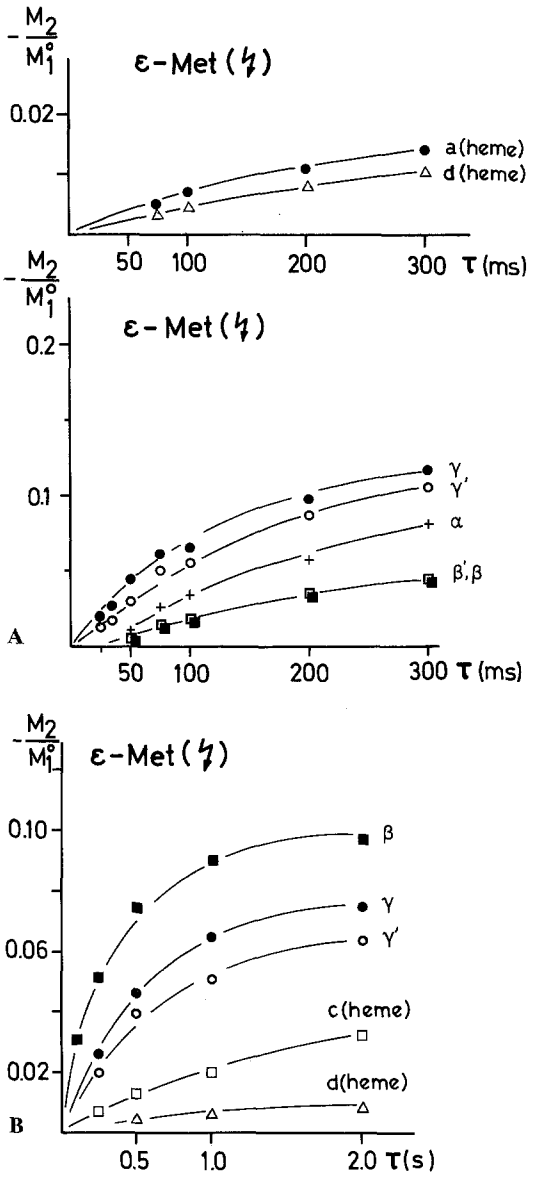

Fig. 4. A NOE build-up curves for individual protons of the heme and the axial methionine in horse ferrocytochrome c obtained from the TOE experiments in Fig. 3, where the preirradiation was on the ε-methyl group of the axial methionine. **B** Same for *P. aeruginosa* ferrocytochrome c 551. The experimental conditions were T = 30° C, 0.006 M protein concentration in ^2H_2O, p^{2}H 7.5, 360 MHz

shows that in both proteins the C^β and C^γ methylene protons are located near the heme meso positions b and c (Fig. 1), whereas the εCH_3 group is near a and d in horse ferrocytochrome c, and near c and d in the *P. aeruginosa* protein (Fig. 4). As a consequence the chirality at the iron-bound sulfur atom must be different in the two proteins (Senn et al. 1980), which in the present study was taken into account by the afore-mentioned choice of the covalent structures for the heme c-Met complexes in the two species. Third, Fig. 4 shows that in horse ferrocytochrome c the C^γ methylene protons are nearer to εCH_3 than the β methylene group, whereas in *P. aeruginosa* ferrocytochrome c-551 the closer distance is between $C^\beta H_2$ and εCH_3. Figure 6 indicates further that in both proteins the closest ^{1}H-^{1}H distances between the two methionine methylene groups are from Hβ to Hγ, and from Hβ' to Hγ', respectively.

For most build-up curves (Figs. 4–6) one observes a slight curvature at very short γ 's, i.e., between 0 and approximately 25 ms. This arises because in practice the equilibrium magnetization on spin 1 is not attained instantaneously (Wagner and Wüthrich 1979). In Fig. 4A the induction period for the NOE build-up on the C^α proton is, however, much longer, indicating that spin diffusion makes a dominant contribution as compared to the direct cross-relaxation with εCH_3. This data was therefore not further used in the quantitative analysis.

Empirical correlation between NOE's and ^1H-^1H distances

As a first step towards a quantitative interpretation of the NOE data, the cross-relaxation rates, σ_{ij}, between the different pairs of protons were evaluated from the

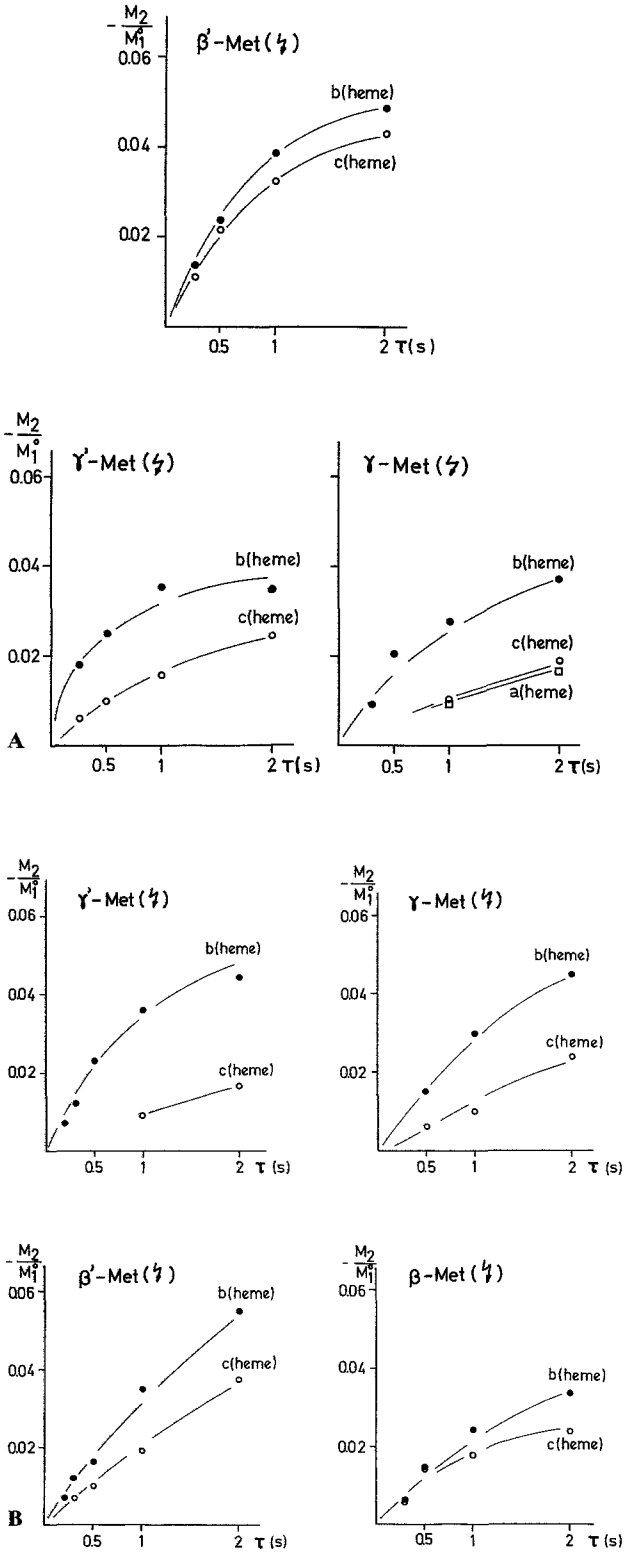

Fig. 5. A NOE build-up curves for the heme meso protons (Fig. 1) of horse ferrocytochrome c after preirradiation of individual methylene protons of the axial methionine (indicated by an arrow). The experimental conditions were T = 30° C, 0.006 M protein concentration in ^2H_2O, p^{2}H 7.2, 500 MHz. **B** Same for *P. aeruginosa* ferrocytochrome c 551. Experimental conditions: T = 30° C, 0.006 M protein concentration in ^2H_2O, p^{2}H 7.2, 500 MHz

Table 1. Cross-relaxation rates σ_{ij} and distances d_{ij} between different protons of the axial methionine and heme c in horse ferrocytochrome c

Presaturated resonance[a]	NOE observed on resonance[a]	Cross-relaxation rate $\sigma(s^{-1})$	^1H-^1H distance d_{ij} (Å)[b]
Met 80 γ'	Met 80 γ	8.5	1.75[b]
	Met 80 β'	1.4	2.4
	Met 80 β	1.0	2.5
	Met 80 α	1.7	2.3
	Met 80 ε	0.4	2.9
	Heme b	0.07	3.8
	Heme c	0.02	4.8
Met 80 γ	Met 80 γ'	8.9	1.75[b]
	Met 80 β'	1.1	2.5
	Met 80 β	1.6	2.3
	Met 80 α	1.1	2.5
	Met 80 ε	0.5	2.8
	Heme b	0.04	4.3
	Heme c	0.01	5.4
Met 80 β'	Met 80 β	8.6	1.75[b]
	Met 80 γ'	1.5	2.3
	Met 80 γ	1.1	2.5
	Met 80 α	2.1	2.2
	Met 80 ε	0.2	3.3
	Heme b	0.04	4.3
	Heme c	0.04	4.3
Met 80 ε	Met 80 γ'	0.6	2.7
	Met 80 γ	0.7	2.6
	Met 80 β'	0.2	3.3
	Met 80 β	0.2	3.3
	Heme a	0.03–0.06	4.0–4.5
	Heme d	0.01–0.04	4.3–5.4
Heme a	Met 80 ε	0.05	4.1
Heme d	Met 80 ε	0.03	4.5
Heme b	Met 80 α	0.1–0.2	3.3–3.5
Heme c	Met 80 α	0.1–0.2	3.3–3.5

[a] For the Cβ and Cγ methylene protons the higher field line in the reduced protein was arbitrarily labelled β' and γ', respectively

[b] The fixed distance between geminal methylene protons was used for distance calibration of the experimental cross-relaxation rates

data in Figs. 4–6 with the use of Eq. (4) and listed in Tables 1 and 2. Many of the σ_{ij} values appear twice in the tables, since they were measured both by irradiation of spin i and observation of spin j, and vice versa. In all cases close coincidence of the different measurements of the same cross-relaxation rate was obtained (Tables 1 and 2).

Proton-proton distances corresponding to the cross-relaxation rates were obtained on the following basis. The distance between the two protons of a methylene group is known to be 1.75 Å. With this information the correlation function $f(\tau_c)$ in Eq. (3) can be evaluated from the σ_{ij} values for methylene

Table 2. Cross-relaxation rates σ_{ij} and distances d_{ij} between different protons of the axial methionine and heme c in *P. aeruginosa* ferrocytochrome c 551

Presaturated resonance[a]	NOE observed on resonance[a]	Cross-relaxation rate $\sigma_{ij}(s^{-1})$	^1H-^1H distance d_{ij} (Å)[b]
Met 61 γ'	Met 61 γ	4.2	1.75[b]
	Met 61 β'	0.6	2.4
	Met 61 β	0.5	2.5
	Met 61 α	0.7	2.4
	Met 61 ε	0.1	3.3
	Heme b	0.04	3.8
	Heme c	0.01	4.8
Met 61 γ	Met 61 γ'	4.1	1.75[b]
	Met 61 β'	0.6	2.4
	Met 61 β	0.8	2.3
	Met 61 α	0.3	2.7
	Met 61 ε	0.1	3.3
	Heme b	0.03	4.0
	Heme c	0.01	4.8
Met 61 β'	Met 61 β	4.2	1.75[b]
	Met 61 γ'	0.5	2.5
	Met 61 γ	0.4	2.6
	Met 61 α	0.5	2.5
	Heme b	0.04	3.8
	Heme c	0.02	4.3
Met 61 β	Met 61 β'	4.5	1.75[b]
	Met 61 γ'	0.5	2.5
	Met 61 γ	0.9	2.3
	Met 61 α	0.3	2.8
	Met 61 ε	0.2	2.9
	Heme b	0.02	4.3
	Heme c	0.02	4.3
Met 61 ε	Met 61 γ'	0.08	3.4
	Met 61 γ	0.1	3.3
	Met 61 β	0.3	2.7
	Heme c	0.03	4.0
	Heme d	0.01	4.8
Heme b	Met 61 α	0.1–0.2	2.9–3.3
Heme c	Met 61 α	0.1	3.3
Heme c	Met 61 ε	0.03	4.0
Heme d	Met 61 ε	0.01	4.8

[a] For the Cβ and Cγ methylene protons the higher field line in the reduced protein was arbitrarily labelled β' and γ', respectively

[b] The fixed distance between geminal methylene protons was used for distance calibration of the experimental cross-relaxation rates

protons. In both proteins identical effective correlation times were thus found for the C$^\beta$ and C$^\gamma$ protons, with $\tau_c \approx 4.5 \cdot 10^{-9}$ s. Therefore ^1H-^1H distances for all combinations of pairs of protons i and j originating from heme c or the axial methionine can to a good approximation be determined relative to the distance between the methionine methylene protons by

$$\frac{\sigma_{\beta\beta'}}{\sigma_{ij}} = \frac{r_{ij}^6}{r_{\beta\beta'}^6} . \qquad (7)$$

The ^1H-^1H distances thus obtained are listed in Tables 1 and 2 for the two proteins.

Structural interpretation of the NOE distance constraints

A direct, unique structural interpretation of the data in Tables 1 and 2 cannot be given, since on the basis of the ^1H-NMR measurements alone the resonances of the methylene protons of the axial methionine cannot be stereospecifically assigned (Wüthrich et al. 1983). The four possible assignments A, B, C, and D for the two pairs of methylene protons are defined in the first two columns of Table 3. For each of the four stereospecific assignments a conformer was determined which would satisfy the NOE distance constraints of Table 1 or Table 2. The following three principal guidelines were used in the interactive computer graphic search for these conformers. (*i*) The chirality at the methionine sulfur atom was fixed at the outset, i.e., R for horse ferrocytochrome c and S for *P. aeruginosa* ferrocytochrome c-551, as described in the preceding sections. (*ii*) In addition to the NOE distance constraints, it is known for both proteins that $^3J_{\alpha\beta} \gtrsim 10$ Hz and $^3J_{\alpha\beta'} \lesssim 3$ Hz (Senn 1983). Hence, Hβ must be *cis* or *trans* to C$^\alpha$H. A cis orientation can be excluded from the NOE data. Therefore the torsion angle χ^1 for the axial methionine was fixed near the value corresponding to *trans* orientation of the protons C$^\alpha$H and Hβ. (*iii*) When fitting the molecular conformations to the experimental distance constraints, account was taken of the fact that with the presently used experimental approach the discrimination between the relative lengths of any two ^1H-^1H distances can be more reliably determined than the absolute values for individual distances (see below).

The conformers obtained with the above procedures are characterized in Table 3 (last two columns) by the dihedral angles χ^1, χ^2, χ^3, and Ω, and by the chirality at the methionine sulfur. Tables 4 and 5 list the distance constraints from the NOE experiments and the corresponding ^1H-^1H distances in the conformers of Table 3. Two important conclusions result from inspection of Tables 4 and 5. First, satisfactory fits of the NOE data could at this point, where the atoms have been treated as dimensionless points and no steric constraints were considered, be achieved for all four stereospecific assignments A, B, C, and D (Table 3). Second, while the short distances agree quite closely, the longer distances in the molecular structures characterized in Table 3 show generally larger deviations from the experimental values. This is due primarily to the fact that spin diffusion is more likely to affect the measurements of the longer

Table 3. The four conformations of the axial methionine in horse ferrocytochrome c and *P. aeruginosa* ferrocytochrome c 551 determined from the NOE distance constraints with the assumption of the four different possible stereospecific ^{1}H-NMR assignments A–D for the β and γ methylene protons. The atoms were treated as dimensionsless points so that no van der Waals constraints were considered

Stereo-specific assignment	Proton[a]	NMR line[b]	Dihedral angles in the methionine side chain[c]									
			Horse ferrocytochrome c					*P. aeruginosa* ferrocytochrome c 551				
			χ^1	χ^2	χ^3	Ω	Met Sδ chirality	χ^1	χ^2	χ^3	Ω	Met Sδ chirality
A	Hβ2	β										
	Hβ1	β'	−172	− 46	−143	133	R	−175	− 47	119	138	S
	Hγ2	γ										
	Hγ1	γ'										
B	Hβ2	β'										
	Hβ1	β	− 56	−163	−161	133	R	− 54	−165	− 60	139	S
	Hγ2	γ										
	Hγ1	γ'										
C	Hβ2	β										
	Hβ1	β'	164	145	140	130	R	166	148	40	139	S
	Hγ2	γ'										
	Hγ1	γ										
D	Hβ2	β'										
	Hβ1	β	− 50	25	128	133	R	− 56	34	28	139	S
	Hγ2	γ'										
	Hγ1	γ										

[a] See Fig. 1. According to Hanson (1966) Hβ1 and Hγ1 would be "pro-S", Hβ2 and Hγ2 "pro-R"

[b] The higher field β and γ methylene ^{1}H-NMR lines are arbitrarily labelled β' and γ' (Fig. 2)

[c] Definition of the dihedral angles χ^1, χ^2, and χ^3 according to the IUPAC/IUB convention (1970). Ω is the dihedral angle about the iron-sulfur bond. Its values are determined by the relative positions of the bond Cγ-S and Fe-N4 (see Fig. 1)

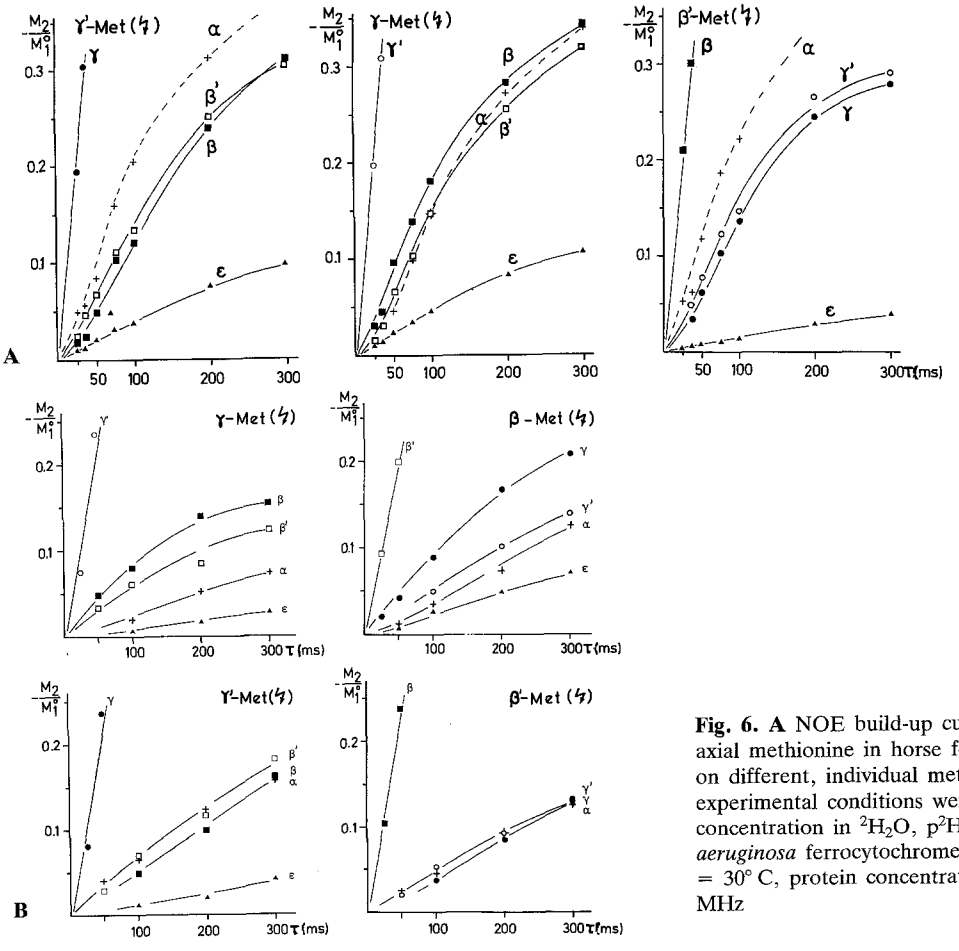

Fig. 6. A NOE build-up curves for individual protons of the axial methionine in horse ferrocytochrome c after preirradiation on different, individual methionine protons (arrows). The experimental conditions were T = 30° C, 0.006 M protein concentration in ^2H_2O, p^{2}H 7.2, 500 MHz. **B** Same for *P. aeruginosa* ferrocytochrome c 551. Experimental conditions: T = 30° C, protein concentration 0.006 M in ^2H_2O, p^{2}H 7.2, 500 MHz

Table 4. ^{1}H-^{1}H distances in the four methionine conformations of horse ferrocytochrome c in Table 3, which were obtained from best fits to the NOE distance constraints using the different stereospecific assignments A–D for the methionine methylene protons. The atoms were treated as dimensionless points so that no van der Waals constraints were considered

^{1}H-NMR lines[a]		NOE distance[b] d_{ij} (Å)	Distance in the molecular structures[c]			
i	j		A	B	C	D
γ'	β'	2.4	2.4	2.6	2.8	2.3
γ'	β	2.5	3.0	3.0	3.0	3.0
γ'	α	2.3	2.7	2.5	2.6	3.0
γ'	ε	2.9	3.6	3.3	3.6	3.7
γ	β	2.3	2.4	2.4	2.3	2.3
γ	β'	2.5	2.6	3.0	3.0	2.7
γ	α	2.5	3.7	3.3	3.7	3.8
γ	ε	2.8	2.9	3.0	2.8	2.8
β'	α	2.2	2.5	2.5	2.4	2.4
β'	ε	3.3	5.1	4.8	4.6	4.3
β	ε	3.3	4.4	4.7	4.5	5.1
ε	a	4.3	4.1	4.1	4.0	4.1
ε	d	4.9	5.4	5.4	5.5	5.4
α	b	3.4	4.5	5.0	3.7	5.0
α	c	3.4	2.9	5.3	4.4	2.6
γ'	b	3.9	5.4	5.5	3.6	3.5
γ'	c	4.8	5.2	5.5	5.4	5.3
γ	b	4.3	4.8	4.5	5.3	5.2
γ	c	5.4	6.3	6.2	6.1	6.2
β'	b	4.3	2.5	4.0	5.3	4.8
β'	c	4.3	5.3	3.4	3.3	4.9

[a] See Fig. 1. The higher field β and γ methylene ^{1}H-NMR lines are arbitrarily labelled β' and γ'
[b] From Table 1
[c] The four possible stereospecific assignments A–D for the Met β and γ methylene protons are defined in Table 3

Table 5. ^{1}H-^{1}H distances for the four methionine conformations of *P. aeruginosa* ferrocytochrome c 551 in Table 3, which were obtained from best fits to the NOE distance constraints using the different stereospecific assignments A–D for the methionine methylene protons. All atoms were treated as dimensionless points so that no van der Waals constraints were considered

^{1}H-NMR lines[a]		NOE distance[b] d_{ij} (Å)	Distance in the molecular structures[c]			
i	j		A	B	C	D
γ'	β'	2.4	2.4	2.6	2.7	2.4
γ'	β	2.5	3.0	3.0	3.0	3.0
γ'	α	2.4	2.7	2.5	2.6	2.9
γ'	ε	3.4	2.8	2.9	4.0	4.0
γ	β'	2.5	2.6	3.1	3.0	2.7
γ	β	2.3	2.4	2.4	2.3	2.3
γ	α	2.7	3.8	3.3	3.6	3.8
γ	ε	3.3	3.8	3.9	3.4	3.5
β'	α	2.5	2.5	2.5	2.4	2.5
β	α	2.8	3.0	3.0	3.0	3.0
β	ε	2.9	4.8	4.6	2.9	2.8
ε	c	4.0	4.2	4.2	4.2	4.2
ε	d	4.8	5.1	5.1	5.1	5.1
α	b	3.1	3.5	4.3	2.8	3.8
α	c	3.3	3.6	5.9	5.5	3.3
γ'	b	3.8	5.1	5.3	3.7	3.6
γ'	c	4.8	5.5	5.8	6.1	6.0
γ	b	4.0	5.0	4.7	5.4	5.3
γ	c	4.8	6.7	6.7	6.5	6.6
β'	b	3.8	3.0	3.3	4.3	4.3
β'	c	4.3	6.1	4.1	3.8	5.5
β	b	4.3	2.7	2.4	5.5	5.8
β	c	4.3	6.2	5.6	5.2	5.4

[a] See Fig. 1. The higher field β and γ methylene ^{1}H-NMR lines are arbitrarily labelled β' and γ'
[b] From Table 2
[c] The four possible stereospecific assignments A–D for the Met β and γ methylene protons are defined in Table 3

distances, and possibly also to the overall reduced accuracy because of the poorer signal-to-noise ratio for measurements of the weak NOEs corresponding to longer distances. Contributions to the NOE intensity from spin diffusion tend to yield systematically short values for ^{1}H-^{1}H distances, a trend which is readily apparent when the experimental values for the longer distances in Tables 4 and 5 are compared with the corresponding distances in the molecular structures which satisfy the shorter distance constraints.

Discrimination between different stereospecific resonance assignments from van der Waals constraints and ring current shifts

A unique structure resulted when in the conformers obtained with the four possible resonance assignments A–D (Table 3) each atom was represented by a sphere, as indicated in the legend to Table 6, and those conformers were eliminated which included sizeable steric constraints. In both proteins only the structure corresponding to the resonance assignments C was thus found acceptable (Tables 6 and 7).

Independent support for the stereospecific resonance assignments C was obtained from a comparison of the experimental chemical shifts of the axial methionine proton lines with the shifts expected from ring current calculations using the atomic coordinates of the four conformers of Table 3. The data are presented in Fig. 7. It is readily apparent that none of the conformers A, B, or D would give rise to similar chemical shifts to those observed, whereas qualitative agreement prevails between the experiment and the shifts predicted for conformer C.

Stereo drawings of heme c and the axial methionine in horse ferrocytochrome c and in *P. aeruginosa* ferrocytochrome c-551 are presented in Fig. 8. Table 8 affords a comparison with the corresponding

Table 6. Van der Waals violations larger than 0.50 Å in the four local structures A–D of horse ferrocytochrome c described in Table 3. The following van der Waals radii, *r*, have been used: C, 1.6 Å; N, 1.45 Å; O, 1.35 Å; S, 1.7 Å; H, 1.0 Å; M, 1.8 Å; L, 1.6 Å; Fe, 1.7 Å (see Fig. 1 and text)

Stereospecific assignment[a]	Interacting atoms[b]		d_{ij} (Å)[c]	$r_i + r_j$ (Å)	$r_i + r_j - d_{ij}$
	i	*j*			
A	N	N3	1.99	2.90	0.91
	N	12	1.37	3.05	1.68
	N	5	0.55	3.05	2.50
	N	6	1.23	3.05	1.82
	N	13	1.91	3.05	1.14
	N	5 C1	1.89	3.25	1.36
	C′	N4	2.37	3.05	0.68
	C′	14	2.43	3.20	0.77
	C′	FE	1.75	3.30	1.55
	Hβ2	11	1.89	2.60	0.71
	Cβ	b	2.61	3.20	0.59
	Hβ2	b	1.80	2.60	0.80
	Cα	N3	1.61	3.05	1.44
	C′	N3	0.85	3.05	2.20
	Cβ	12	2.35	3.20	0.85
	Hβ2	12	2.09	2.60	0.51
	Cα	12	1.79	3.20	1.41
	C′	12	2.06	3.20	1.14
	Cα	5	1.98	3.20	1.22
	Hα	6	2.04	2.60	0.56
	Cα	6	1.98	3.20	1.22
	C′	6	2.59	3.20	0.61
	Hα	13	1.86	2.60	0.74
	Cα	13	1.69	3.20	1.51
	C′	13	1.43	3.20	1.77
	C′	Sδ	2.51	3.30	0.79
	C′	c	2.11	3.20	1.09
B	Hβ1	b	1.86	2.60	0.74
	Cβ	12	2.48	3.20	0.72
	Hβ1	12	1.72	2.60	0.88
	C′	5	2.45	3.20	0.75
	C′	5 C1	1.90	3.40	1.50
C	No violations > 0.5 Å				
D	N	Sδ	2.17	3.15	0.98
	Hα	13	1.96	2.60	0.64
	Cα	Sδ	2.78	3.30	0.52

[a] See Table 3
[b] See Fig. 1
[c] d_{ij} is the interatomic distance in the conformation obtained with the respective stereospecific assignment

crystal structures (Takano and Dickerson 1981; Matsuura et al. 1982). This comparison reveals that the conformations in single crystals and in solution are nearly identical. In view of the limited accuracy of both methods the small deviations of the torsion angles are within the limits of error and should not be taken to be significant.

Table 7. Van der Waals violations larger than 0.50 Å in the four local structures A–D of *P. aeruginosa* ferrocytochrome c 551 described in Table 3. The same van der Waals radii, *r*, were used as in Table 6

Stereospecific assignment[a]	Interacting atoms[b]		d_{ij} (Å)[c]	$r_i + r_j$ (Å)	$r_i + r_j - d_{ij}$
	i	*j*			
A	N	b	1.29	3.05	1.76
	N	Hb	1.61	2.45	0.84
	N	N3	2.10	2.90	0.80
	N	12	0.79	3.05	2.26
	N	5	1.27	3.05	1.78
	N	6	2.44	3.05	0.61
	N	5 C1	2.08	3.25	1.17
	C′	Sδ	2.53	3.30	0.77
	Cβ	11	2.47	3.20	0.73
	Cβ	b	2.41	3.20	0.79
	Cβ	12	2.55	3.20	0.65
	Hβ2	11	1.67	2.60	0.93
	Hα	N3	1.78	2.45	0.67
	Hα	12	1.87	2.60	0.73
	Hα	13	1.94	2.60	0.66
	Cα	FE	2.77	3.30	0.53
	Cα	11	2.59	3.20	0.61
	Cα	b	1.96	3.20	1.24
	Cα	N3	1.47	3.05	1.58
	Cα	12	1.28	3.20	1.92
	Cα	5	2.13	3.20	1.07
	Cα	6	2.57	3.20	0.63
	Cα	13	2.29	3.20	0.91
	C′	FE	1.32	3.30	1.98
	C′	N2	2.18	3.05	0.87
	C′	11	2.57	3.20	0.63
	C′	b	2.43	3.20	0.77
	C′	N3	0.81	3.05	2.24
	C′	12	1.77	3.20	1.43
	C′	13	2.08	3.20	1.12
B	Cβ	b	2.57	3.20	0.63
	Cβ	12	2.47	3.20	0.73
	Hβ1	11	1.77	2.60	0.83
	Hβ1	b	1.72	2.60	0.88
	Hβ2	N3	1.92	2.45	0.53
	Hβ2	12	1.95	2.60	0.65
	C′	5 C1	2.72	3.40	0.68
C	No violation > 0.5 Å				
D	N	Mε	1.47	3.25	1.78
	N	Sδ	2.28	3.15	0.87
	Cβ	Mε	1.14	3.40	2.26
	Hβ1	Mε	1.28	2.80	1.52
	Hβ2	Mε	2.14	2.80	0.66
	Hα	Mε	2.05	2.80	0.75
	Hα	N3	1.81	2.45	0.64
	Hα	6	2.09	2.60	0.51
	Hα	13	1.79	2.60	0.81
	Cα	Mε	1.15	3.40	2.25
	Cα	13	2.48	3.20	0.72
	C′	6 C2	2.25	3.20	0.95
	C′	Mε	2.13	3.40	1.27

[a] See Table 3
[b] See Fig. 1
[c] d_{ij} is the interatomic distance in the conformation obtained with the respective stereospecific assignment

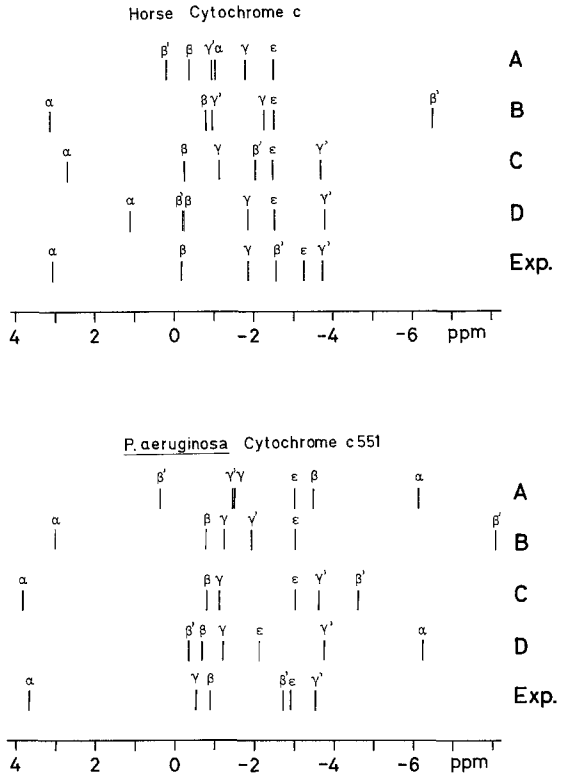

Fig. 7. Comparison of the experimental ^{1}H-NMR chemical shifts for the axial methionine in horse ferrocytochrome c and *P. aeruginosa* ferrocytochrome c 551 with the chemical shifts computed for the four molecular structures obtained by interpreting the NOE distance constraints with the four possible stereospecific assignments A–D for the methionine methylene protons (Table 3). The computed shifts are the sum of the random coil shifts (Bundi and Wüthrich 1979) and the ring current shifts due to the heme group (see text)

Table 8. Comparison of the torsion angles which characterize the conformation of the axial methionine (Fig. 1) in the solution and crystal conformations of horse ferrocytochrome c and *P. aeruginosa* ferrocytochrome c 551

	Solution conformation (NMR)	Single crystal conformation (X-ray)[a]
Horse ferrocytochrome c	$\chi_1 = 164°$ $\chi_2 = 145°$ $\chi_3 = 140°$ $\Omega = 130°$	$\chi_1 = 169°$ $\chi_2 = 164°$ $\chi_3 = 145°$ $\Omega = 143°$
P. aeruginosa ferrocytochrome c 551	$\chi_1 = 166°$ $\chi_2 = 148°$ $\chi_3 = 40°$ $\Omega = 139°$	$\chi_1 = 176°$ $\chi_2 = 166°$ $\chi_3 = 44°$ $\Omega = 136°$

[a] The dihedral angles in the crystal structures were computed using coordinates from the Protein Data Bank (Bernstein et al. 1977) for tuna ferrocytochrome c (Takano and Dickerson 1981) and *P. aeruginosa* cytochrome c 551 (Matsuura et al. 1982)

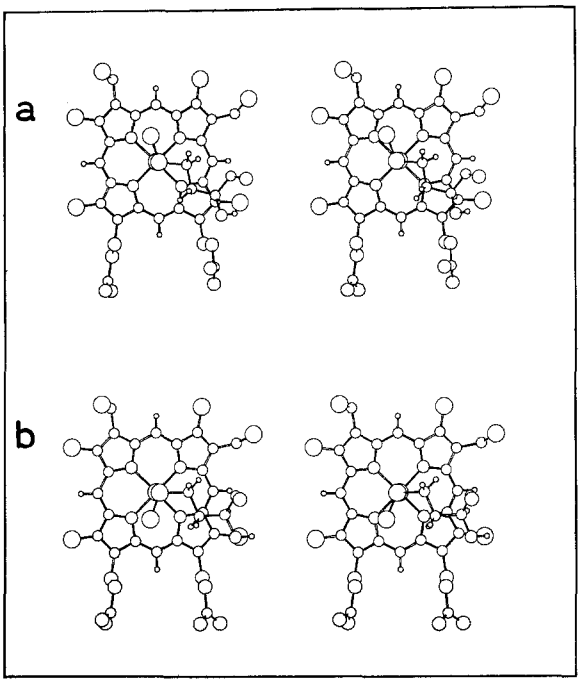

Fig. 8a and b. Computer drawings affording stereo presentations of the heme group and the axial methionine in the solution structures of horse ferrocytochrome c (**a**) and *P. aeruginosa* ferrocytochrome c 551 (**b**) determined by combined use of NMR and computer graphics. As in Fig. 1 the methyl groups and most methylene groups are represented by equivalent spheres

Conclusions

The method used here for the determination of the conformation of the axially bound methionine is generally applicable for c-type cytochromes. Since it is known that the electronic structure of the heme in oxidized cytochromes c is largely governed by the spatial arrangement of the axial methionine (Senn et al. 1980, 1983a, b; Senn and Wüthrich 1983a, b, c), detailed studies of a variety of species are of considerable interest. X-ray studies of single crystals can also provide this structural information, but since NMR can focus exclusively on the immediate heme environment of the proteins it is a more efficient technique for this special purpose.

The present study represents an illustration of refinement of a local protein conformation determined by NMR which can result when stereospecific assignments for amino acid side chains are obtained during the later stages of the work from reference to nearby hydrogen atoms in the spatial structure (Wüthrich et al. 1983). In the place of a heme group other structure elements might serve as points of reference, for example β-sheets or helical segments.

For work with more complex structural problems the presently used techniques may have to be substituted by more elaborate procedures. When the resonance lines of interest are not well separated in the ^{1}H-NMR spectrum, two-dimensional NOE spectroscopy (NOESY) (Anil Kumar et al. 1980) may be used instead of TOE difference spectroscopy. The manual real-time interactive approach to structure determination becomes quite impractical when the number of conformational variables increases, and it may then become advisable to combine its use with that of automated procedures (Braun et al. 1981, 1983).

Acknowledgements. Financial support was obtained from the Schweizerischer Nationalfonds (projects 3.528.79 and 3.284.82) and through a special grant of the Eidgenössische Technische Hochschule (ETH) Zürich. Use of the facilities at the Zentrum für Interaktives Rechnen of the ETH is gratefully acknowledged. We thank Dr. W. Braun for helpful discussions in the early phases of the project, Dr. I. Gunsalus and Dr. P. Debrunner for a gift of *P. aeruginosa* ferricytochrome c-551 and Mrs E. Huber for the careful preparation of the manuscript.

References

Anil Kumar, Ernst RR, Wüthrich K (1980) A two-dimensional nuclear Overhauser enhancement (2D NOE) experiment for the elucidation of complete proton-proton cross-relaxation networks in biological macromolecules. Biochem Biophys Res Commun 95: 1–6

Anil Kumar, Wagner G, Ernst RR, Wüthrich K (1981) Buildup rates of the nuclear Overhauser effect measured by two-dimensional proton magnetic resonance spectroscopy: implications for studies of protein conformation. J Am Chem Soc 103: 3654–3658

Bernstein FC, Koetzle TF, Williams GJB, Meyer EF Jr., Brice MD, Rodgers JR, Kennard O, Shimanouchi T, Tasumi M (1977) The protein data bank: a computer-based archival file for macromolecular structures. J Mol Biol 112: 535–542

Billeter M (1980) Computerunterstützter graphischer Modellbau von Polypeptidketten unter Berücksichtigung von NMR-Daten. Diploma Thesis, Institut für Molekularbiologie, ETH-Zürich

Bothner-By AA, Noggle JH (1979) Time development of nuclear Overhauser effects in multispin systems. J Am Chem Soc 101: 5152–5155

Braun W, Bösch Ch, Brown LR, Gō N, Wüthrich K (1981) Combined use of proton-proton Overhauser enhancements and a distance geometry algorithm for determination of polypeptide conformations. Applications to micelle-bound glucagon. Biochim Biophys Acta 667: 377–396

Braun W, Wider G, Lee KH, Wüthrich K (1983) Conformation of glucagon in a lipid-water interphase by ^{1}H nuclear magnetic resonance. J Mol Biol 169: 921–948

Bundi A, Wüthrich K (1979) ^{1}H NMR parameters of the common amino acid residues measured in aqueous solutions of the linear tetrapeptides H-Gly-Gly-X-L-Ala-OH. Biopolymers 18: 285–298

Diamond R (1978) BILDER, An inter-active graphics program for biopolymers, users' guide, MRC Laboratory of Molec. Biol., Hills Road, Cambridge, England

Dobson CM, Olejniczak ET, Poulsen FM, Ratcliffe RG (1982) Time development of proton nuclear Overhauser effects in proteins. J Magn Reson 48: 97–110

Dubs A, Wagner G, Wüthrich K (1979) Individual assignments of amide proton resonances in the proton NMR spectrum of the basic pancreatic trypsin inhibitor. Biochim Biophys Acta 577: 177–194

Giessner-Prettre C, Pullman B (1971) Intermolecular nuclear shielding due to the aromatic amino acids of proteins and to porphyrins. J Theor Biol 31: 287–294

Gordon SL, Wüthrich K (1978) Transient proton-proton Overhauser effects in horse ferrocytochrome c. J Am Chem Soc 100: 7094–7096

Hanson KR (1966) Applications of the sequence rule. I. Naming the paired ligands g,g at a tetrahedral atom xggis. II. Naming the two faces of a trigonal atom yghi. J Am Chem Soc 88: 2731–2742

IUPAC-IUB Commission on Biochemical Nomenclature (1970) Abbreviations and symbols for the description of the conformation of polypeptide chains. J Mol Biol 52: 1–17

Johnson CE, Bovey FA (1958) Calculation of nuclear magnetic resonance spectra of aromatic hydrocarbons. J Chem Phys 29: 1012–1014

Kalk A, Berendsen HJC (1976) Proton magnetic relaxation and spin diffusion in proteins J Magn Reson 24: 343–366

Keller RM, Wüthrich K (1978a) Assignment of the heme c resonances in the 360 MHz ^{1}H NMR spectra of cytochrome c. Biochim Biophys Acta 533: 195–208

Keller RM, Wüthrich K (1978b) Evolutionary change of the heme c electronic structure: ferricytochrome c-551 from *Pseudomonas aeruginosa* and horse heart ferricytochrome c. Biochem Biophys Res Commun 83: 1132–1139

Keller RM, Wüthrich K (1981) Multiple irradiation a^{1}H NMR experiments with hemoproteins. In: Berliner LJ, Reuben J (eds) Biological magnetic resonance, vol 3. Plenum Press, New York London, pp 1–52

Keller RM, Schejter A, Wüthrich K (1980) ^{1}H NMR studies of the coordination geometry at the heme iron and the electronic structure of the heme group in cytochrome c-552 from *Euglena gracilis*. Biochim Biophys Acta 626: 15–22

Matsuura Y, Takano T, Dickerson RE (1982) Structure of cytochrome c_{551} from *Pseudomonas aeruginosa* refined at 1.6Å resolution and comparison of the two redox forms. J Mol Biol 156: 389–409

Moore GE, Williams RJP (1980) Nuclear-magnetic-resonance studies of eukaryotic cytochrome c. Eur J Biochem 130: 493–502

Noggle JH, Schirmer RE (1971) The nuclear Overhauser effect. Academic Press, New York

Olejniczak ET, Poulsen FM, Dobson CM (1981) Proton Nuclear Overhauser Effects and Protein Dynamics J Am Chem Soc 103: 6574–6580

Perkins SJ (1980) Ring current models for the heme ring in cytochrome c. J Magn Reson 38: 297–312

Senn H (1983) Zusammenhänge zwischen Aminosäuresequenz, Haem-Eisen-Koordinationsgeometrie und funktionellen Eigenschaften in Cytochromen c: ^{1}H-NMR Studien. Ph. D. Thesis, Nr. 7314, ETH-Zürich

Senn H, Wüthrich K (1983a) Individual ^{1}H-NMR assignments for the heme groups and the axially bound amino acids and determination of the coordination geometry at the heme iron in a mixture of two isocytochromes c-551 from *Rhodopseudomonas gelatinosa*. Biochim Biophys Acta 743: 69–81

Senn H, Wüthrich K (1983b) Conformation of the axially bound ligands of the heme iron and electronic structure of heme c in the cytochromes c-551 from *Pseudomonas mendocina* and *Pseudomonas stutzeri* and in cytochrome c_2 from *Rhodospirillum rubrum*. Biochim Biophys Acta 746: 48–60

Senn H, Wüthrich K (1983c) A new spatial structure for the axial methionine observed in cytochrome c_5 from *Pseudomonas mendocina*. Correlations with the electronic structure of heme c. Biochim Biophys Acta 747: 16–25

Senn H, Keller RM, Wüthrich K (1980) Different chirality of the axial methionine in homologous cytochromes c determined by ^{1}H NMR and CD spectroscopy. Biochem Biophys Res Commun 92: 1362–1369

Senn H, Eugster A, Wüthrich K (1983a) Determination of the coordination geometry at the heme iron in three cytochromes c from *Saccharomyces cerevisiae* and from *Candida krusei* based on individual ^{1}H-NMR assignments for heme c and the axially coordinated amino acids. Biochim Biophys Acta 743: 58–68

Senn H, Guerlesquin F, Bruschi M, Wüthrich K (1983b) Coordination of the heme iron in the low-potential cytochromes c-553 from *Desulfovibrio vulgaris* and *Desulfovibrio desulfuricans*. Different chirality of the axially bound methionine in the oxidized and reduced states. Biochim Biophys Acta 748: 194–204

Solomon I (1955) Relaxation processes in a system of two spins. Phys Rev 99: 559–565

Takano T, Dickerson RE (1981) Conformation change of cytochrome c. I. Ferrocytochrome c structure refined at 1.5Å resolution. J Mol Biol 153: 79–94

Wagner G, Wüthrich K (1979) Truncated driven nuclear Overhauser effect (TOE). A new technique for studies of selective ^{1}H-^{1}H Overhauser effects in the presence of spin diffusion. J Magn Reson 33: 675–680

Wüthrich K, Billeter M, Braun W (1983) Pseudo-structures for the 20 Common amino acids for use in studies of protein conformations by measurements of intramolecular proton-proton distance constraints with nuclear magnetic resonance. J Mol Biol 169: 949–961